Institute of Pharmaceutics[1], Zhejiang University, Hangzhou, Zhejiang, P. R. China; Department of Pharmaceutical Sciences[2], University of Tennessee Health Science Center, Memphis, USA; Zhejiang-California International Nanosystems Institute Molecular Imaging Platform[3], Zhejiang University, Hangzhou, Zhejiang, P. R. China

Cellular uptake and elimination of lipophilic drug delivered by nanocarriers

XIAOYI SUN[1], FENG LI[2], YE WANG[3], WENQUAN LIANG[1]

Received April 5, 2010, accepted April 25, 2010

Prof. Wenquan Liang, Institute of Pharmaceutics, Zhejiang University, 388 Yuhangtang Road, Hangzhou, 310058, P. R. China
wqliang@zju.edu.cn

Pharmazie 65: 737–742 (2010) *doi: 10.1691/ph.2010.0099*

To investigate the cellular uptake and elimination process of a lipophilic drug loaded in different nanocarriers, emulsions, liposomes and poly (DL-lactide-co-glycolide) (PLGA) nanoparticles loaded with a model drug, coumarin 6, were prepared and their transportation in HeLa cells compared. After 4 h incubation, liposomes and nanoparticles mediated significantly higher intracellular drug levels, which were 3 or 2.5 times that of the emulsion group, into cells. A novel kinetic model was established to analyze the cellular elimination process. Emulsions had the longest intracellular mean residence time (MRT), which was about 1-2 times longer than other nanocarriers. The endocytosis inhibition experiment suggested that the coumarin 6 in liposomes and nanoparticles entered cells directly via diffusion, while part of the intracellular coumarin 6 was taken up through clathrin-mediated endocytosis in emulsions. Combined with the results on uptake pathway and kinetic parameters, it can be concluded that different nanocarriers bring about diverse mechanisms of cellular uptake and elimination.

1. Introduction

Pharmaceutical nanocarriers such as emulsions, liposomes and biodegradable nanoparticles have been employed extensively for the delivery of poorly water soluble drugs. The use of nanocarriers makes it possible to target drugs into tumors through the enhanced permeability and retention (EPR) effect, which is important for cancer chemotherapy. On arriving at the target site, nanocarriers may release their payloads outside the cells (Gullotti and Yeo 2009) or enter into cells and unload drugs at the desired intracellular locations (Breunig et al. 2008; Torchilin 2006).

Drug release properties of nanocarriers can be controlled by appropriate design of their composition, architecture, and particle size. Drug substances loaded in different nanocarriers are intended to exhibit different pharmacokinetic profiles and biodistributions (Li and Huang 2008; Alexis et al. 2008; Yang and Benita 2000). Interactions between carriers and cells also can be changed (Peetla and Labhasetwar 2008; Vasir and Labhasetwar 2008). Are there any cellular trafficking differences between commonly used nanocarriers? How to make an optimal choice among these available nanocarriers becomes a considerable issue. Until now, only a limited number of studies (Dhanikula et al. 2005; Saad et al. 2008) have been reported which compare drug cellular delivery mediated with different nanocarriers under similar experimental conditions. Many of them put emphasis on uptake enhancement, but efforts to explore drug elimination are less frequent. Since nanocarriers are widely applied to drug delivery systems for antitumor agents with low solubility, we chose human cervical cancer cell (HeLa) as a model cell line to investigate the uptake and elimination process. In this study, we established a kinetic model to describe the cellular elimination process and compared the differences in cellular uptake and elimination of lipophilic coumarin 6 loaded in emulsions, liposomes, and PLGA nanoparticles. The mechanisms of drug release and cellular uptake were also investigated.

2. Investigations and results

2.1. Characterization of nanocarriers

The mean diameters for the emulsions, liposomes and PLGA nanoparticles were 228.4 ± 10.5, 212.8 ± 8.6 and 265 ± 9.7 nm, respectively. All of them displayed modest negative zeta potential ranging from -2.5 mV to -12.8 mV.

In vitro release of these nanocarriers is shown in Fig. 1. Drug release from liposomes was rapid. Emulsion gave the slowest release among these carriers.

2.2. Cellular uptake and elimination kinetics

Cellular uptake kinetic experiments were carried out at the same concentration of coumarin 6 (1 μg/ml) loaded in nanocarriers. Cumulative cellular uptake of coumarin 6 over time is shown in Fig. 2(A). Cellular uptake increased with time and reached a plateau within 1.5 h except for the nanoparticle group. The liposome group had the highest coumarin 6 intracellular level followed by nanoparticles. Results showed that emulsions had the poorest ability to transport this lipophilic drug into cells, with a cellular coumarin 6 level only 30% of that in the liposome group.

Cellular drug delivery was observed with a confocal microscope after incubating HeLa cells with nanoparticles (Fig. 3(A)). A similar intracellular distribution of coumarin 6 was observed for all nanocarriers (data not shown). Coumarin 6 was located

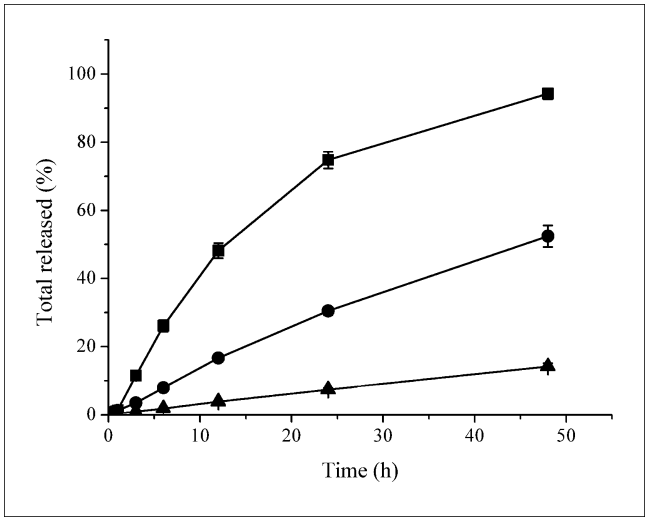

Fig. 1: *In vitro* release of coumarin 6 from different nanocarriers. (■) Liposomes; (●) Nanoparticles; (▲) Emulsions. Data are expressed as mean ± S.D of four independent experiments

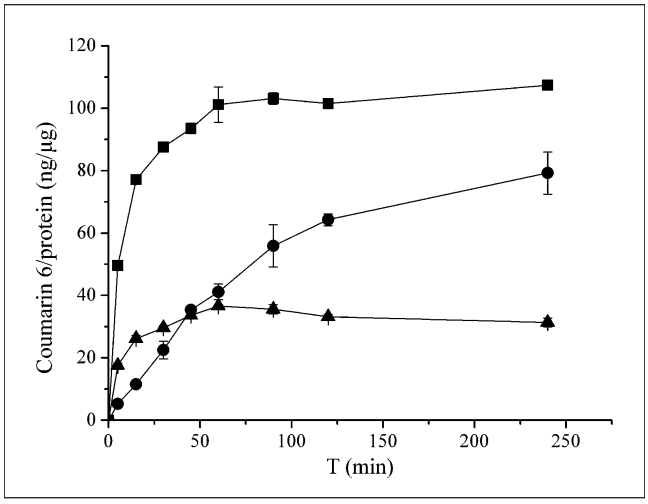

(A)

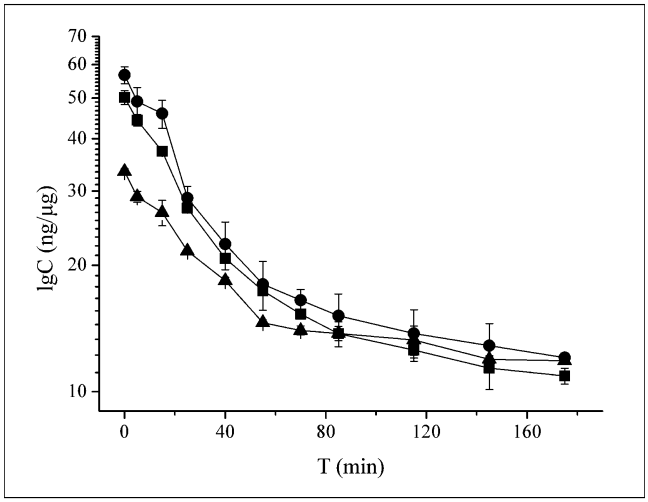

(B)

Fig. 2: Kinetics of coumarin 6 uptake and elimination in HeLa cells delivered with different nanocarriers. (A) Cellular uptake. Cells incubated with 1 μg/ml coumarin 6 loaded nanocarriers for defined lengths of time. Cells then washed and lysed for assay of coumarin 6. (B) Cellular elimination. Cells incubated with nanocarriers first and then drug-containing medium replaced by drug-free medium. After eliminating for defined time periods, lysis products of cells collected. (■) Liposomes; (●) Nanoparticles; (▲) Emulsions

extensively in cytoplasm but isolated by nuclear membrane. In the elimination process, intracellular fluorescent intensity decreased. The kinetic results are shown in Fig. 2(B). Elimination rate was high in the first hour and about 60% of the initial coumarin 6 was cleared. However, the elimination rate decreased significantly in the following two hours. The bright perinuclear region disappeared and fluorescence dispersed extensively in cytoplasm after elimination for one hour. Intracellular distributions were recorded before and after coumarin 6 elimination (Fig. 3(B)).

In order to describe the initially fast and then slow elimination process quantitatively, it is assumed that the drug distributes into compartments A and B in a typical cell (Fig. 3(C)). The drug diffuses rapidly into compartment A and has stronger affinity and slow equilibration with compartment B. This model assumes that the drug is eliminated from compartment A. Eq. (1) describes drug transfer between compartment A, compartment B and the extracellular medium, where C_A and C_B are the drug concentrations in compartment A and B, respectively, and k_{10}, k_{12} and k_{21} are the rate constants of drug transfer from compartment A to the medium, from compartment A to B, and from compartment B to A, respectively.

$$\frac{dC_A}{dt} = k_{21}C_B - k_{12}C_A - k_{10}C_A \tag{1}$$

Eq.2 represents the transfer between compartment A and compartment B:

$$\frac{dC_B}{dt} = k_{12}C_A - k_{21}C_B \tag{2}$$

Solving Eq. (1) and Eq. (2) gives Eqs. (3) and (4), which describe the changes in drug concentration in the two compartments with respect to time, where C_0 is the initial cellular drug concentration, and α and β are hybrid elimination rate constants which could represent the fast and slow elimination processes.

$$C_A = \frac{C_0(\alpha - k_{21})}{\alpha - \beta} \cdot e^{-\alpha t} + \frac{C_0(k_{21} - \beta)}{\alpha - \beta} \cdot e^{-\beta t} \tag{3}$$

$$CB = \frac{k_{12}C_0}{\alpha - \beta}(e^{-\beta t} - e^{-\alpha t}) \tag{4}$$

$$\alpha = \frac{(k12 + k21 + k10) + \sqrt{(k_{12} + k_{21} + k_{10})^2 - 4k_{21} \cdot k_{10}}}{2}$$

$$\beta = \frac{(k_{12} + k_{21} + k_{10}) - \sqrt{(k_{12} + k_{21} + k - 10)^2 - 4k_{21} \cdot k_{10}}}{2}$$

Combining Eq. (3) and (4) a simple biexponential Eq. (5) which describes the cellular elimination kinetics of the drug is obtained, where C is the intact cellular level at time point t. The sum of constants a and b is the drug concentration when $t = 0$.

$$C = C_A + C_B = a \cdot e^{-\alpha t} + b \cdot e^{-\beta t} \tag{5}$$

$$a = \frac{C_0(\alpha - k_{21} - k_{12})}{\alpha - \beta}$$

$$b = \frac{C_0(k_{21} - \beta + k_{12})}{\alpha - \beta}$$

Kinetic parameters including α, β, $t_{1/2(\alpha)}$, $t_{1/2(\beta)}$ and *MRT* are listed in the Table. All groups shared a similar fast elimination rate constant α, while emulsions had a minimal β value and a maximum *MRT* which was 1-2 times longer than the other two groups.

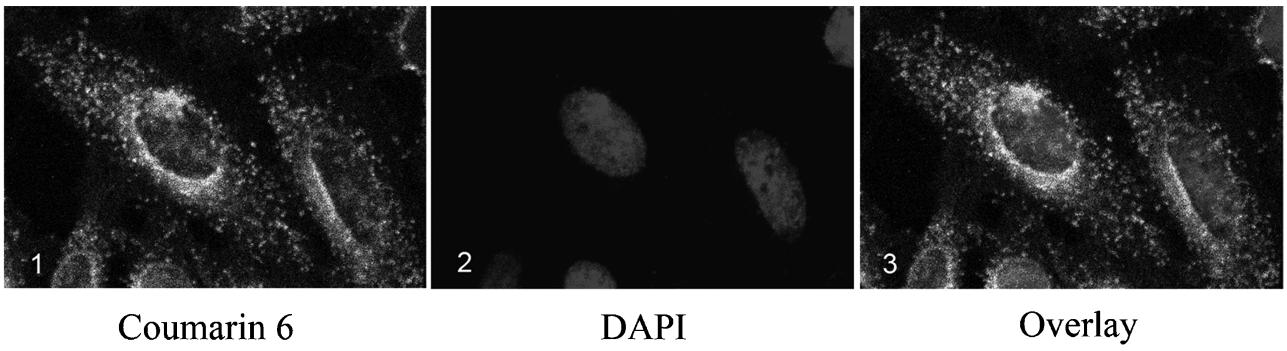

(A)

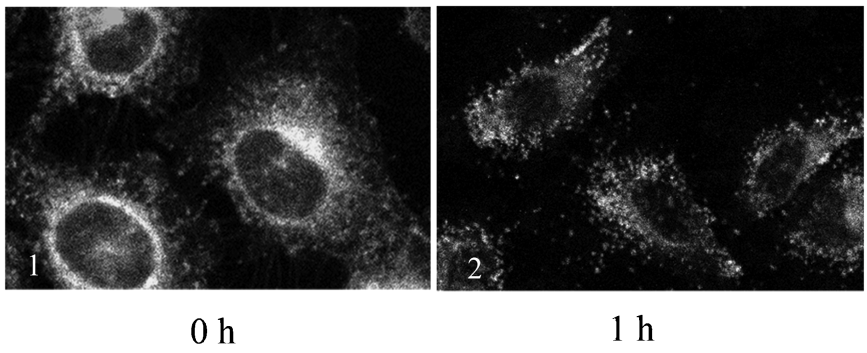

(B)

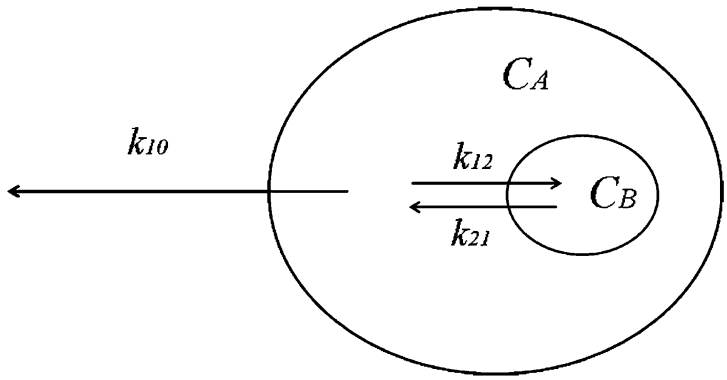

(C)

Fig. 3: Intracellular delivery of coumarin 6. (A) Intracellular drug distribution observed by confocal microscopy. Cells incubated with courmain 6 loaded PLGA nanoparticles for 30 min. Cells stained by DAPI to visualize cell nucleus (1. FITC channel; 2. DAPI channel; 3.merged). (B) Fluorescence microscopic images of HeLa cells during elimination process (1. Starting point of elimination; 2. One hour elimination in culture medium). (C) Scheme of drug elimination process analyzed with two-compartment model

Table: Cellular elimination parameters for coumarin 6 nanocarriers

	$\alpha(h^{-1})$	$\beta(10^{-2} \times h^{-1})$	$t_{1/2(\alpha)}$ $(10^{-2} \times h)$	$t_{1/2(\beta)}$(h)	*MRT*(h)
Emulsions	2.07 ± 0.08	4.26 ± 0.52	33.57 ± 1.31	16.45 ± 2.02	23.04 ± 2.89
Liposomes	2.39 ± 0.29	10.79 ± 2.56*	29.31 ± 3.54	6.70 ± 1.74**	8.74 ± 2.32**
Nanoparticles	2.49 ± 0.23	9.75 ± 1.45**	27.97 ± 2.57	7.21 ± 1.07**	9.42 ± 1.45**

*$p < 0.05$, **$p < 0.01$ compared with parameters of emulsion group

2.3. Inhibition of cellular uptake

Endocytosis inhibition was studied to find out whether the nanocarriers entered into cells and unloaded the drug or released the drug outside the cells. The requirement for metabolic energy in cellular uptake was probed by incubating cells with the glycolysis inhibitors 2-deoxyglucose/ sodium azide (2DG/NaN_3). Clathrin-mediated endocytosis was inhibited by the pharmacological inhibitors chlorpromazine (CPZ) or sucrose leading to hypertonic conditions. The uptake of coumarin 6 delivered by emulsions was significantly inhibited by 2DG/ NaN_3, CPZ and sucrose ($p < 0.05$). However, inhibitors had little effects on the cellular drug concentrations delivered by the other two nanocarriers (Fig. 4(A)).

Endocytosis is a dose-dependent process which can be saturated by increased nanocarrier concentration. To study the cellular uptake mechanism further, Hela cells were preincubated with a high dosage of blank nanocarriers (no cytotoxicity was observed as determined by MTT) for 2 h before the cellular uptake experiment. If cellular uptake were

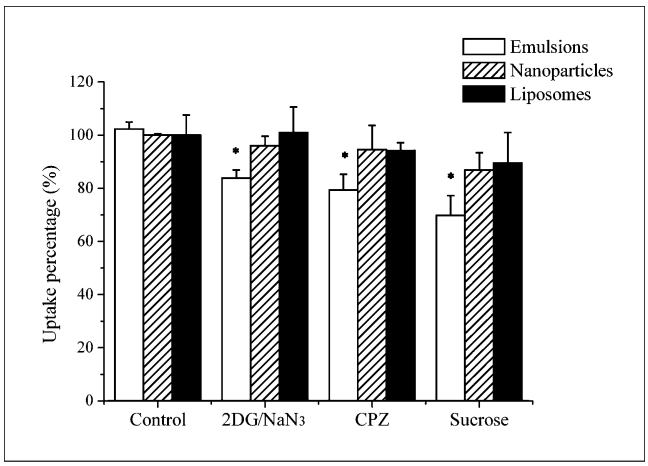

(A)

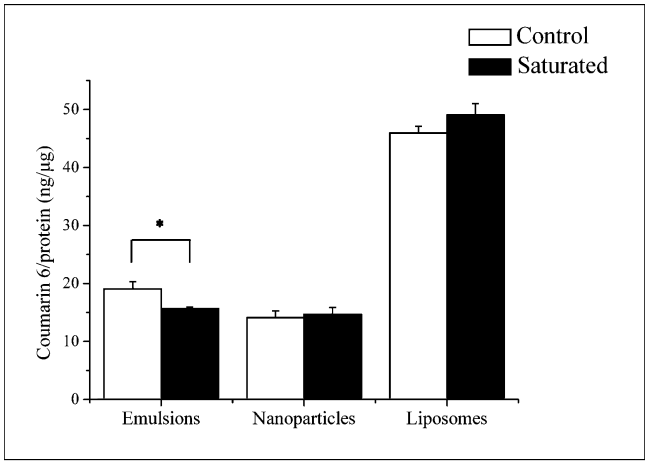

(B)

Fig. 4: Inhibition of coumarin 6 cellular uptake in HeLa cells. (A) Effect of endocytosis inhibitors on cellular uptake (*$p < 0.05$ compared with respective nanocarrier control). (B) Effect of pre-saturation with blank nanocarriers (*$p < 0.05$ compared with control). Data expressed as mean ± S.D of 3-4 independent experiments

through endocytosis, pre-incubation with blank nanocarriers would reduce the total cellular uptake. Otherwise, if the drug molecules diffused through the cellular membrane, the pre-saturated blank nanocarriers would have a negligible effect on cellular uptake. After pre-incubation with blank nanocarriers, the intracellular coumarin 6 level was significantly decreased in the emulsion group ($p < 0.05$, Fig. 4(B)).

3. Discussion

One of the main routes for small molecules to enter into cells is through passive diffusion. Lipid-soluble drugs can diffuse readily. Coumarin 6 is permeable with a large partition coefficient (logP 6.9). Endocytosis inhibition results indicated that nanoparticles and liposomes delivered payloads to cells mainly by drug release and/or direct drug transfer to the contacted cells, which is consistent with the findings of Xu et al. (2009) and Pietzonka et al. (2002). With emulsions, both passive diffusion and endocytosis contributed to cellular uptake. The CPZ and sucrose inhibition results indicated that the endocytosis of emulsions was mainly through a clathrin-mediated pathway. Endocytosis pre-saturation with blank nanocarriers confirmed the results obtained by uptake inhibitors above.

In view of the major contribution of diffusion/contact transfer to drug uptake, the drug release rate might determine the cellular drug content. Thus, uptake kinetics correspond to *in vitro* release rates with these carriers. Faster release from the nanocarrier meant more drug would be delivered into cells. Coumarin 6 release from PLGA nanoparticles was much faster than the degradation of the polymer. From this standpoint, drug release might not be controlled by erosion of the polymer, but be mainly due to drug diffusion through the pores and channels inside the nanoparticles (Yeo and Park 2004). The fast releasing liposomes and nanoparticles tended to deliver coumarin 6 to cells passively through diffusion, so that endocytosis could be ignored. In contrast, the hydrophobic drug was prone to be retained in the oil phase of emulsions which enabled the contribution of endocytosis to be observed. So the sustained release emulsions had the lowest power to deliver the drug into cells.

Although the endocytosis of nanocarriers did not play a predominant role in coumarin 6 cellular delivery, it should be noted that in emulsions around 20% of cellular uptake was still accomplished via endocytosis. This modest percentage would result in significant differences in the subsequent cellular elimination process.

The heterogeneous intracellular distribution of coumarin 6 caught our attention. The staining of the perinuclear region staining especially punctuated as was previously observed with another lipophilic probe, Nile Red (Xu et al. 2009). The pronounced fluorescence near the nucleus at the concave side probably corresponded to the Golgi apparatus and the endoplasmic reticulum as with hypericin in A431 cells (Vandenbogaerde et al. 1998) at the end of uptake. During the elimination period, the bright perinuclear region gradually disappeared. The heterogeneous intracellular distribution, in other words, the different drug affinity for various intracellular components, was probably the main reason for the biphasic elimination process. As was discussed above, free coumarin 6 mainly transferred from liposomes and nanoparticles to cells, but some of the coumarin 6 was taken up within emulsions. Once the external concentration gradient disappeared, drug molecules would diffuse out from cells incubated with liposomes and nanoparticles. However, it would be different in the emulsion group. After one hour of rapid elimination, the elimination constant β was significantly smaller than in the other two groups. The high intracellular retention ability might be attributed to internalized emulsions. As with many lipophilic drugs, amphiphilic protein can enhance solubility. In our pre-experiment, we observed an albumin solubilization effect on coumarin 6. The extremely high concentration of intracellular protein might solubilize coumarin 6 and cause the drug to be released from emulsion droplets inside the cells. Elimination then occurred as the drug diffused out. Another possibility which we suggest might cause the slow elimination in the emulsion group is emulsion exocytosis. Part of the nanocarriers internalized by clathrin-mediated endocytosis are reported to be exocytosed out of cells (Park et al. 2006; Huth et al. 2007). Compared with diffusion elimination, this is an energy-consuming and slow process. Sustained delivery of the drug inside cells has also been observed with other nanoparticles (Chavanpatil et al. 2007).

4. Experimental

4.1. Materials

Coumarin 6 and cholesterol were purchased from Sigma (St. Louis, MO, USA). Soya phosphatidylcholine (SPC) and lecithin Lipoid E-80 were provided by Lipoid GmbH (Ludwigshafen, Germany). PLGA, lactic to glycolic acid molar ratio 50:50 (Mw 20KDa) was purchased from Shandong Medical Instrumental Institute (China). Sodium azide (NaN_3) and 2-deoxyglucose (2DG) were bought from Acros Organics (New Jersey, USA). Ploxamer188 was purchased from BASF (Germany). Soybean oil and CPZ injection were kindly donated

by Tieling Beiya Medical Oil Co., Ltd. (Tielin, Liaoning, China) and Yatai Huashi Pharmaceutical Co., Ltd (Changchun, Jilin, China), respectively. Dulbecco's modified Eagle's medium (DMEM), trypsin and penicillin-streptomycin were purchased from Gibco BRL (Gaithersberg, MD, USA). Fetal bovine serum (FBS) was purchased from Sijiqing Biologic Co., Ltd. (Hangzhou, China). BCA protein assay kit was supplied by Beyotime Biotechnology (Jiangsu, China). HeLa cells were purchased from the Institute of Biochemistry and Cell Biology, Shanghai Institute for Biological Sciences, Chinese Academy of Sciences. All other chemicals were of analytical grade.

4.2. Preparation and characterization of nanocarriers

The emulsions were prepared as described previously (Zhao et al. 2007) with slight modifications. The formulation (%, w/w) consisted of soybean oil (10), Lipoid E-80 (1.5) and glycerol (2.25). Coumarin 6 was first dissolved in the oil phase with a final concentration of 30 μg/ml in emulsions. Liposomes were prepared by thin lipid film hydration followed by sonication and extrusion as described previously (Chen et al. 2007). The formulation consisted of 5 mg/ml soya phosphatidylcholine, 2.5 mg/ml cholesterol and 30 μg/ml coumarin 6. PLGA nanoparticles were prepared using an emulsion-solvent evaporation technique (Davda and Labhasetwar 2002).

The particle size and zeta potential of the nanocarriers were determined by laser diffraction spectrometry (Malvern Zetasizer 3000HS, Malvern, UK).

To determine coumarin 6 release prior to cellular uptake, *in vitro* drug release was monitored using a dialysis method. Nanocarriers loaded with 5 μg coumarin 6 were suspended in 0.5 ml phosphate-buffered saline (PBS) and placed in a dialysis bag (MWCO: 14 kDa). The dialysis bag was placed in a receiving compartment filled with 50 ml PBS containing 0.5% Tween 80 and shaken at 37 °C, 75 strokes/min. Two milliliters of medium were sampled for fluorescence intensity measurement and an equal volume of fresh medium was replaced at the times indicated.

4.3. Cell experiment

HeLa cells were maintained in DMEM supplemented with 10% (v/v) FBS, 100 IU/ml penicillin and 100 IU/ml streptomycin in a humidified incubator (95% air, 5% CO_2) at 37 °C.

To determine cellular coumarin 6 uptake, HeLa cells were seeded at 1×10^5 cells/well in 24-well plates and allowed to attach overnight. Cells were incubated with nanocarriers in growth medium at a concentration of 1 μg/ml coumarin 6 for various lengths of time. Then the cells were washed thoroughly with PBS and lysed by 0.2 ml cell culture lysis reagent. The samples were examined by fluorescence intensity for assay of coumarin 6. For the drug elimination study, cells were incubated with coumarin 6 nanocarriers first, then the drug-containing medium was replaced by the drug-free medium. After elimination for the defined time periods, cells were thoroughly washed and lysed using the protocol described above.

The energy dependence of nanocarrier-cell interactions was assessed using 2DG/ NaN_3. Briefly, HeLa cells were incubated in 50 mM 2DG/0.05% NaN_3 in DMEM containing 10% FBS for 1 h, and then incubated with coumarin 6 (1 μg/ml) loaded nanocarriers for 30 min. A clathrin-mediated endocytosis inhibition test (Hartig et al. 2007; Huang et al. 2002) was done by pre-incubating Hela cells with 10 μg/ml CPZ for 30 min. before addition of coumarin 6 (1 μg/ml) loaded nanocarriers. The endocytosis saturation experiment was conducted using pre-uptake treatment with blank nanocarriers. Cells were pre-incubated with blank nanocarriers for 2 h, then coumarin 6 (1 μg/ml) loaded nanocarriers were added. The cell lysate was collected 5 min. after incubation. The control group was exposed to coumarin 6 loaded nanocarriers at the same concentration without pre-treatment with inhibitors or saturation.

4.4. Assay of coumarin 6

Plates containing 0.1 ml/well cell lysate were taken for fluorescence intensity measurements using a Microplate Reader (Tecan Infinite M200, Switzerland) with excitation wavelength of 456 nm and emission wavelength of 504 nm (Goldstein et al. 2007; Win and Feng 2005). Cells incubated with blank nanocarriers served as background intensity and were used as the negative control.

Total protein was determined by a BCA protein assay kit. Intracellular coumarin 6 level in each well was normalized by protein concentration.

4.5. Confocal laser scanning microscopy (CLSM)

For CLSM, HeLa cells were seeded at 1×10^5 cells/well in 24-well plates and allowed to attach overnight. Courmain 6 loaded nanocarriers (1 μg/ml) were added and incubated for 30 min. After removal of nanocarriers, cells were fixed by 4% paraformaldehyde and stained with DAPI to visualize the cell nucleus. For cell observation after drug elimination, cells were incubated in drug-free medium for 1 h after 30 min. uptake. The plate was then placed on the stage of a confocal microscope (LSM 410, Zeiss, Germany). Representative cells were selected at random and pictures were taken with FITC and DAPI filters.

4.6. Statistical analysis

All values are presented as mean ± S.D from 3-4 independent measurements for all control and experimental data points. Statistical analysis was performed using a two-tailed, Student's *t* test assuming equal variance in groups. Kinetica™ V.4.4 pharmacokinetics software was utilized to analyze cellular drug elimination.

Acknowledgments: This study was supported by the National Nature Science Foundation of China (No. 30873176, No.30701058). The authors are grateful to the Laboratory Center at the Institute of Pharmaceutics, Zhejiang University for technical support.

References

Alexis F, Pridgen E, Molnar LK, Farokhzad OC (2008) Factors affecting the clearance and biodistribution of polymeric nanoparticles. Mol Pharm 5: 505-515.

Breunig M, Bauer S, Goefferich A (2008) Polymers and nanoparticles: Intelligent tools for intracellular targeting? Eur J Pharm Biopharm 68: 112–128.

Chavanpatil MD, Khdair A, Panyam J (2007) Surfactant-polymer nanoparticles: A novel platform for sustained and enhanced cellular delivery of water-soluble molecules. Pharm Res 24: 803–810.

Chen JL, Wang H, Gao JQ, Chen HL, Liang WQ (2007). Liposomes modified with polycation used for gene delivery: Preparation, characterization and transfection *in vitro*. Int J Pharm 343: 255–261.

Davda J, Labhasetwar V (2002) Characterization of nanoparticle uptake by endothelial cells. Int J Pharm 233: 51–59.

Dhanikula AB, Singh DR, Panchagnula R (2005) *In vivo* pharmacokinetic and tissue distribution studies in mice of alternative formulations for local and systemic delivery of paclitaxel: gel, film, prodrug, liposomes and micelles. Curr Drug Deliv 2: 35–44.

Goldstein D, Sader O, Benita S (2007) Influence of oil droplet surface charge on the performance of antibody-emulsion conjugates. Biomed Pharmacother 61: 97–103.

Gullotti E, Yeo Y (2009) Extracellularly activated nanocarriers: a new paradigm of tumor targeted drug delivery. Mol Pharm 6: 1041–1051.

Hartig SM, Greene RR, Carlesso G, Higginbotham JN, Khan WN, Prokop A, Davidson JM (2007) Kinetic analysis of nanoparticulate polyelectrolyte complex interactions with endothelial cells. Biomaterials 28: 3843–3855.

Huang M, Ma ZS, Khor E, Lim LY (2002) Uptake of FITC-chitosan nanoparticles by a549 cells. Pharm Res 19: 1488–1494.

Huth US, Schubert R, Peschka-Süss R (2007) Spectral imaging for the investigation of the intracellular fate of liposomes. In: Gregoridadis G (ed.) Liposomes technology, 3rd ed., New York, p. 341–372.

Li SD, Huang L (2008) Pharmacokinetics and biodistribution of nanoparticles. Mol Pharm 5: 496–504.

Park JS, Han TH, Lee KY, Han SS, Hwang JJ, Moon DH, Kim SY, Cho YW (2006) N-acetyl histidine-conjugated glycol chitosan self-assembled nanoparticles for intracytoplasmic delivery of drugs: endocytosis, exocytosis and drug release. J Control Release 28: 37–45.

Peetla C, Labhasetwar V (2008) Biophysical characterization of nanoparticle-endothelial model cell membrane interactions. Mol Pharm 5: 418–429.

Pietzonka P, Rothen-Rutishauser B, Langguth P, Wunderli-Allenspach H, Walter E, Merkle HP (2002) Transfer of lipophilic markers from PLGA and polystyrene nanoparticles to Caco-2 monolayers mimics particle uptake. Pharm Res 19: 595–601.

Saad M, Garbuzenko OB, Ber E, Chandna P, Khandare JJ, Pozharov VP, Minko T (2008) Receptor targeted polymers, dendrimers, liposomes: Which nanocarrier is the most efficient for tumor-specific treatment and imaging? J Control Release 130: 107–114.

Torchilin VP (2006) Recent approaches to intracellular delivery of drugs and DNA and organelle targeting. Annu Rev Biomed Eng 8: 343–375.

Vandenbogaerde AL, Delaey EM, Vantieghem AM, Himpens BE, Merlevede WJ, de Witte PA (1998) Cytotoxicity and antiproliferative effect of hypericin and derivatives after photosensitization. Photochem Photobiol 67: 119–125.

Vasir JK, Labhasetwar V (2008) Quantification of the force of nanoparticle-cell membrane interactions and its influence on intracellular trafficking of nanoparticles. Biomaterials 29: 4244–4252.

Win KY, Feng SS (2005) Effects of particle size and surface coating on cellular uptake of polymeric nanoparticles for oral delivery of anticancer drugs. Biomaterials 26: 2713–2722.

Xu PS, Gullotti E, Tong L, Highley CB, Errabelli DR, Hasan T, Cheng JX, Kohane DS, Yeo Y (2009) Intracellular drug delivery by poly(lactic-co-glycolic acid) nanoparticles, Revisited. Mol Pharm 6: 190–201.

Yang SC, Benita S (2000) Enhanced absorption and drug targeting by positively charged submicron emulsions. Drug Develop Res 50: 476–486.

Yeo Y, Park KN (2004) Control of encapsulation efficiency and initial burst in polymeric microparticle systems. Archives Pharm Res 27: 1–12.

Zhao YX, Gao JQ, Sun XY, Chen HL, Wu LM, Liang WQ (2007) Enhanced nuclear delivery and cytotoxic activity of hydro-xycamptothecin using o/w emulsions. J Pharm Pharm Sci 10: 61–70.